CSI Based High Accuracy Device Free Passive Localization System

YugeLiu, Wenhui Xiong, *Member, IEEE,* Zhaowei Zhu, and Shaoqian Li, *Fellow, IEEE*

***Abstract*—A new radio frequency fingerprint that incorporates the channel impulse response and Angle of Arrival was introduced to enhance the accuracy of the indoor positioning. To use the new fingerprint. We use the generalized distance metric, i.e., Jensen-Shannon Divergence and cluster center to compare the difference between data collected at the test point and given reference point. Based on the new RF fingerprint, we proposed a device free passive localization system that does not require the user to have any measurement devices. The user location is estimated by searching the reference points with the the smallest distance between the test data and the database. The experimental result shows that the proposed system has better location accuracy method comparing with the conventional fingerprint algorithms.**

***Index Terms*—Indoor Positioning, Channel Impulse Response, AoA, RF Fingerprint**

I. Introduction

POSITION information plays an important role in location based services (LBS). The indoor positioning is a challenging task due to the weak satellite signal and multipath effect. Many radio based systems e.g., [1]–[7] were proposed to address this challenge. All these systems are device dependent systems, where the measurements is taken by the device carried by the entity to be located. This may limit the application of these systems. The device free passive localization (DFPL) system, on the other hand, does not put any requirements on the entity to be located, but relies on the fact that the RF signal is affected by the entity in the monitored area. Some researchers proposed to use the widely available WIFI network for DFPL, e.g., Real Time Indoor Localization(RTI) [8], which uses large number of WIFI links to infer the position of the person in the monitored area. In this paper, we proposed a DFPL system that utilizes the fine grained physical layer information of WIFI signal. The WIFI system uses OFDM modulation, where the channel's frequency response (CFR) can be estimated by the pilot subcarriers. The channel's CFR, denoted by channel state information (CSI), provides rich information regrading the multipath channel between the transmitter and the receiver. Specifically, because of the rich multipath for indoor environment, people at different locations will affect the propagation differently. As a result, the CSI observed at the receiver will be different, and the people's location can be inferred accordingly. Our proposed DFPL system used the CSI reported by the off the shelf network interface card (NIC) during the normal communication. The CSI is processed to estimate the multipath channel information for building fingerprint database and user position estimation.

The rest of this paper is organized as follows. In section II, we review the related works. In section III, we present our system architecture, how the CSI is precessed to generate the fingerprint database, and the process needed for training and online localization. In Section IV we present the experimental results of our proposed DFPL system.

II. Related Works

The indoor positioning schemes fall into two categories: propagation model based and RF fingerprint. The propagation model based positioning scheme [9], [10] used the fact that the received signal strength (RSS) decreases as the transmitter-receiver distance increases. The propagation based model, however, suffers from the rich multipath for indoor environment where the RSS readings is time and spatial varying, and it is possible to have a lower RSS when the receiver is closer to the transmitter [1]. As a result, the localization accuracy for model based scheme is undesirable.

For RF fingerprint schemes, the RSS values are often used for fingerprint systems. The measured RSS values at the known positions(also known as reference point) are stored to build the fingerprint database. During the localization phase, the user's location is determined by matching the collected RSS with the database. Conventional fingerprint system needs the site survey which is labor intensive. To ease the RF fingerprint database building process many crowd-sourcing based schemes, e.g.,Will [4], Lifi [3], Walkie-Markie [5] were proposed to automatically establish the relationship between the physical location and the measured RSS.

CSI which provides fine grained information of the propagation environment has the potential to improve the indoor positioning accuracy. Wu et al. [1] used the dominant paths from CSI to build the propagation model. The experiment shows great improvement of the range estimation and the position accuracy over the conventional RSS based model. The feasibility of using the CSI as the fingerprint was also studied by many researchers. The CSI fingerprint system proposed by [7], [11] achieve better indoor positioning accuracy than RSS based fingerprint systems. Those CSI based systems are active system, where the user to be located must carry the WIFI devices for CSI measurement.

Our proposed scheme is a DFPL scheme that does not require the user to carry any measurement devices. We use the variation of the multipath channel and AoA information to locate user in the monitored area. Unlike the CSI based passive motion detection schemes [12] [13] , which only tells whether the object is moving in the indoor environment, our proposed scheme is able to provide accurate user location information.

978-1-5386-6358-5/18/$31.00 ©2018 IEEE
Authorized licensed use limited to: University of Electronic Science and Tech of China. Downloaded on July 18,2022 at 08:12:10 UTC from IEEE Xplore. Restrictions apply.

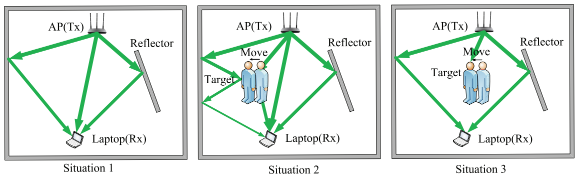

Fig. 1: The variation of CSI caused by blockage

III. System Design

A. Intuition

In a typical indoor environment, there are multiple propagation paths between the transmitter and the receiver. Mathematically, the multipath channel can be expressed as

$$h(t) = \sum_i \alpha_i \delta(t - \tau_i) \tag{1}$$

where α_i and τ_i are respectively the complex amplitude and delay of the ith path of the multipath channel. Let's assume the transmitted signal $x(t)$ is of bandwidth W, with the channel model given by (1), and Nyquist sampling, the discretized received signal can be expressed as

$$y[m] = \sum_l h_l[m] x[m-l] \tag{2}$$

where the lth complex channel filter tap at time m is given by

$$h_l[m] = \sum_i \alpha_i(m/W) sinc[l - \tau_i(m/W)W] \tag{3}$$

As shown in (3), $h_l[m]$ is the result of the the physical propagation paths within the delay bin of width $1/W$. Let's consider the propagation environment of two typical situations shown in Fig. 1. In scenario 1, there is no obstruction between transmitter and receiver, while in scenario 2 there are persons between transmitter and receiver link. Comparing to scenario 1, the obstruction caused by the persons changes multipath channel, e.g., the number of paths and each path's amplitude are different in this case. Therefore, the effective channel model will be different for these 2 cases, and we can use the observed channel model to infer (estimate) where the obstruction is.

B. System Architecture

The architecture of our proposed localization system is shown in fig. 2 where the 802.11n WIFI signal is transmitted by one stationary transmitter. We collected CSI with a laptop equipped with INTEL 5300 Network Interface Card (NIC). The operation of our proposed system can be separated into training and online localization phases. During the training stage, the tested area is divided into small regions of approximately $1m \times 1m$. One person stays in that region for a short period of time to ensure we have collected enough CSI. Then, the person moves to the next region. The process is repeated until the whole test area is covered. The CSIs collected during the training stage are processed to estimated the CIR and AoA information that is needed to build the passive database. During the localization phase, the person stays at a random location within the monitored area. The collected CSI is processed to match with the passive database to estimate the location of the person.

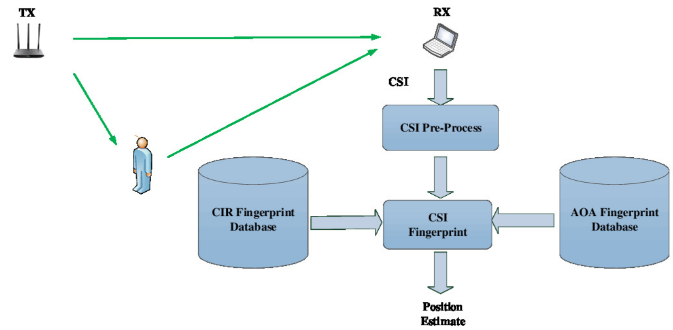

Fig. 2: Proposed System Block Diagram

C. CSI pre-processing

The NIC5300 reports complex CSI of 30 pilot subcarriers. The channel of the kth subcarrier between the ith transmitting antenna and the jth receiving antenna is

$$\hat{H}_{i,j}[k] = H[k] \exp(j\theta) \exp\left(-j2\pi k \frac{T_{i,j}}{N}\right) \Phi_{ij}[k] \tag{4}$$

where $H[k]$ is the composite transmitter-receiver filter's frequency response at the kth subcarrier, θ is the random phase uniformly distributed within the interval $(0, 2\pi)$ to account for the phase offset between the transmitter and receiver oscillator, $T_{i,j}$ is the residual synchronization error which can be modeled as a uniform distribution within $[-1/2, 1/2]$, and $\Phi_{ij}[k] = DFT(h_l[m])$ is the multipath channel's frequency in response to subcarrier k. Normalize $H_{i,j}[k]$ with respect to the $H_{1,1}[k]$ we have

$$\tilde{H}_{i,j}[k] = \frac{\hat{H}_{i,j}[k]}{\hat{H}_{1,1}[k]} = \exp\left(-j2\pi \frac{T_{i,j} - T_{1,1}}{N}\right) \frac{\Phi_{i,j}[k]}{\Phi_{1,1}[k]} \tag{5}$$

The $\tilde{H}_{i,j}[k]$ shown in (5) can be treated as the effective CFR between the ith transmitting antenna and the jth receiving antenna. The exponential term in (5) is the uniformly distributed random noise and can be removed using low pass filter. We applied IDFT to the effective CFR given by (5) to obtain the effective time domain CIR.

$$\tilde{\mathbf{h}}_{i,j}^{(k)} = \text{IDFT}\left(\tilde{\mathbf{H}}_{i,j}^{(k)}\right) \tag{6}$$

As described in previous subsection, the CIR is directly affected by the propagation environment. Fig.3 shows the PDF of the first channel tap's normalized amplitude when a person is at different locations in the test area. As shown in this figure, the PDFs of two different cases are considerably different, which makes our proposed device free localization system possible.

Authorized licensed use limited to: University of Electronic Science and Tech of China. Downloaded on July 18,2022 at 08:12:10 UTC from IEEE Xplore. Restrictions apply.

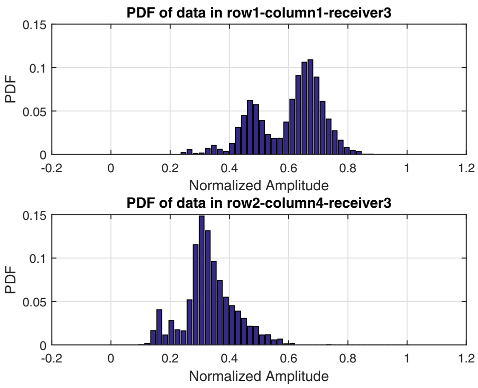

Fig. 3: The PDF of the 1st channel tap's amplitude when the person is at different locations

D. Training

We use CIR and AoA at different reference point to build the RF fingerprint database. CIR database was generated by choosing the higher SNR channel taps where the lower SNR taps were discarded. We denote the PDFs of the lth channel taps between the ith receive antenna and the jth transmit antenna at location k as $\mathbf{q}_{i,j}^{(k)}(l)$, i.e

$$\mathbf{q}_{i,j}^{(k)}(l) = \text{PDF}\left(\left|\tilde{\mathbf{h}}_{i,j}^{(k)}[l]\right|\right) \tag{7}$$

We concatenate the PDFs of L high SNR channel taps of all RF chain as the fingerprint of the location k:

$$\mathbf{Q}_{CIR}^{(k)} = \left[\mathbf{q}_{i,j}^{(k)}(1), \mathbf{q}_{i,j}^{(k)}(2)....\mathbf{q}_{i,j}^{(k)}(L)\right] \tag{8}$$

One reasoning for discarding the lower power channel taps is that the indoor measurement [14] shows that the multipath channel is often sparse in time domain. Therefore, we can use those channel taps with higher SNR to generate the fingerprint without the loss of the information regarding the channel. This will greatly reduce the amount of memory needed for database storage and the complexity of fingerprint matching.

The Angle of Arrival(AoA) and Time of Flight(ToF) is estimated using the algorithm proposed by [15]. Specifically, we can construct smoothed CSI matrix as

$$CSI_{smooth} = \begin{bmatrix} csi_{1,1} & csi_{1,2} & \cdots & csi_{1,16} & csi_{2,1} & \cdots & csi_{2,16} \\ csi_{1,2} & csi_{1,3} & \cdots & csi_{1,17} & csi_{2,2} & \cdots & csi_{2,17} \\ \vdots & \vdots & \vdots & \vdots & \vdots & \vdots & \vdots \\ csi_{1,15} & csi_{1,16} & \cdots & csi_{1,30} & csi_{2,15} & \cdots & csi_{2,30} \\ csi_{2,1} & csi_{2,2} & \cdots & csi_{2,16} & csi_{3,1} & \cdots & csi_{3,16} \\ csi_{2,2} & csi_{2,3} & \cdots & csi_{2,17} & csi_{3,2} & \cdots & csi_{3,17} \\ \vdots & \vdots & \vdots & \vdots & \vdots & \vdots & \vdots \\ csi_{2,15} & csi_{2,16} & \cdots & csi_{2,30} & csi_{3,15} & \cdots & csi_{3,30} \end{bmatrix} \tag{9}$$

where $csi_{i,j}$ is the CSI of the jth subcarrier of the ith antenna. Then the MUSIC spectrum estimation method [15] is applied to estimate the AoA and ToF by obtaining AoA and ToF of multipath components as peaks of MUSIC spectrum.

$$[\mathbf{ToF}_n^{(k)}, \mathbf{AoA}_n^{(k)}] = \mathbf{MUSIC}({CSI_{smooth}}_n^{(k)}) \tag{10}$$

We use K-nearest neighbor (KNN) to cluster the AoAs to obtain the center of each cluster as

$$\mathbf{C}_i^{(k)} = \mathbf{KNN}(\mathbf{AoA}^{(k)}, \mathbf{ToF}^{(k)}) \tag{11}$$

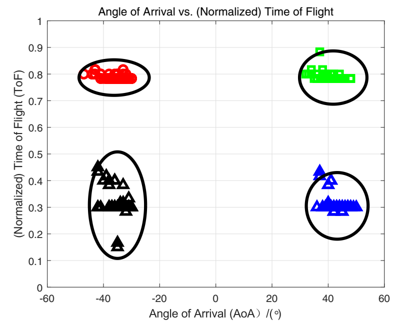

(a) location 1

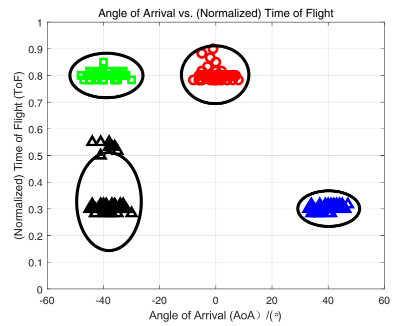

(b) location 2

Fig. 4: AoA/ToF clustering results when the personal is at different locations

where C_i^k is the centroid of the ith cluster at location k. A typical clustering results of AoA at different location is shown in Fig. 4. As shown in this figure, the centroids C_i^k varies when the person is at different location. Thus, we use the centroids to build the AoA fingerpirnt

$$\mathbf{Q}_{AoA}^{(k)} = [\mathbf{C}_1^{(k)}, \mathbf{C}_2^k, ...\mathbf{C}_N^k] \tag{12}$$

Finally, we concatenate $\mathbf{Q}_{CIR}^{(k)}$ and $\mathbf{Q}_{AoA}^{(k)}$ to form the fingerprint for reference point k as

$$\mathbf{Q}^{(k)} = [\mathbf{Q}_{CIR}^{(k)}, \mathbf{Q}_{AoA}^k] \tag{13}$$

E. online localization

During the online positioning phase, the person is at a random location within the monitored area, and the CSI is collected by the stationary laptop. The CSIs are processed following the method described in previous section to obtain the fingerprint of location under test as $\mathbf{Q}^{(t)}$. The MAP approach is then adopted to estimate the person's location, $\mathbf{L}^* = (L_x, L_y)$. Specifically, the user's location $\mathbf{L}^*$ is estimated by maximizing the posterior probability of $P(\mathbf{L}|\mathbf{Q}^{(t)})$.

$$\mathbf{L}^* = \arg\max_{\mathbf{L}} P(\mathbf{L}|\mathbf{Q}^{(t)}) \tag{14}$$

According to Bayes rule, $P(\mathbf{L}|\mathbf{Q}^{(t)})$ can be expressed as

$$P(\mathbf{L}|\mathbf{Q}^{(t)}) = \frac{P(\mathbf{L})P(\mathbf{Q}^{(t)}|\mathbf{L})}{P(\mathbf{Q}^{(t)})} \tag{15}$$

where $P(\mathbf{L})$ is the probability of that the user is at location $P(\mathbf{L})$. Since we have no prior information regarding where

Authorized licensed use limited to: University of Electronic Science and Tech of China. Downloaded on July 18,2022 at 08:12:10 UTC from IEEE Xplore. Restrictions apply.

the user is, we assume that user can be of anywhere within the monitored area, i.e., $P(\mathbf{L})$ follows uniform distribution. It is worth noting that $P(\mathbf{Q}^{(t)})$ conveys no information of user's location, (14) can be expressed as

$$\mathbf{L}^* = \arg\max_{\mathbf{L}} P(\mathbf{Q}^{(t)}|\mathbf{L}) \tag{16}$$

where $P(\mathbf{Q}^{(t)}|\mathbf{L})$ is the likelihood of observing the fingerprint $\mathbf{Q}^{(t)}$ at location $\mathbf{L}$, and it can be interpreted as the similarity, or the distance, between $\mathbf{Q}^{(t)}$ and $\mathbf{Q}^{(k)}$. Since the fingerprint database has two types of features, i.e., CIR and AoA, we use two metrics for evaluating the distances of these two features between the test data and the database.

For CIR test, the Jensen-Shannon Divergence (JSD) is used. The JSD between two distribution P and Q is given by

$$D_{JSD}\left(P \| Q\right) = \frac{1}{2}\sum_i P\left(i\right)\log\frac{P\left(i\right)}{Q\left(i\right)} + \frac{1}{2}\sum_i Q\left(i\right)\log\frac{Q\left(i\right)}{P\left(i\right)} \tag{17}$$

Then, the JSD between the collected CIR when the person is at the random location and the CIR when the person is at the reference point k is

$$D_{CIR}^{(t,k)} = D_{JSD}\left(\mathbf{Q}_{CIR}^{(t)} \middle\| \mathbf{Q}_{CIR}^{(k)}\right) \tag{18}$$

Similarly, we use the AoA centroids to calculate the distance of the AoAs when the person is at the random location and the AoAs when the person is at reference point k as

$$D_{AoA}^{(t,k)} = \sum_i \|(C_i^{(t)} - C_i^{(k)})\| \tag{19}$$

where $C_i^{(t)}$ and $C_i^{(k)}$ denotes the $i$the centroid of clusters at location t and k respectively.

We then normalize the metrics $D_{CIR}^{(t,k)}$ and $D_{AoA}^{(t,k)}$ with respect to their maximum values and use the weighted sum to obtain the distance between the test data the reference point k as.

$$D^{(t,k)} = \lambda_1 \mathbf{D}_{CIR}^{(t,k)} + \lambda_2 D_{AoA}^{(t,k)} \tag{20}$$

The metric distance $D^{(t,k)}$ quantitatively describes the similarity between the fingerprints when the person is at the test location and reference point, the likelihood of observing the fingerprint $\mathbf{Q}^{(t)}$ at the the reference point k is inverse proportional to the similarity between two fingerprints, i.e.,

$$P(\mathbf{Q}^{(t)}|k) \propto \frac{1}{D^{(t,k)}} \tag{21}$$

Plug (21) into (16) we have the estimated user's location as

$$\mathbf{L}^* = \arg\min_{\mathbf{k}\in[1,2,\cdots K]} \prod D^{(t,k)} \tag{22}$$

IV. Experimental Results

A. Implementation

In this section, we present the experimental procedures and the performance of our proposed localization system. The experiment was conducted at a classroom in the university campus. One WIFI AP MW300R was used to transmit WIFI signal. The receiver is a laptop equipped with network interface card (NIC) Intel5300, and the csi-tool [16] is used to collect the CSI. During the experiment, the laptop connects to the AP, and the transmitter-receiver link is configured to work on 2×2 MIMO mode of 20MHz bandwidth at 2.412GHz. The laptops pings AP at 200Hz rate. The test area is shown in Fig.5, where the AP is placed at the font of the classroom and the laptop is placed at the rear row of the classroom. We select 10 reference points for each row for this 9-row classroom. During the online localization phase, one person stands at a random location in the tested area, and the laptop which collects the fingerprint reports the estimated location of the person.

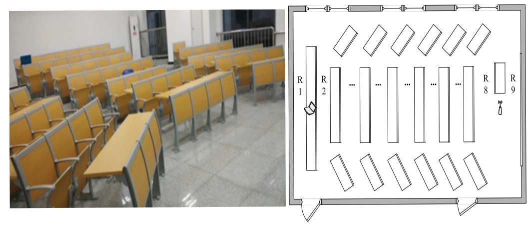

Fig. 5: Experimenter Set

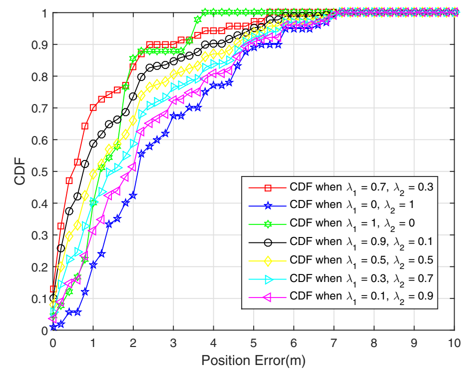

Fig. 6: MAD distribution with different λ_1, λ_2

B. Localization Accuracy

The performance of our proposed system is shown in Fig. 6 where the effects of different λ_1 and λ_2 values were investigated. As shown in this figure, as the value of λ_1 increases from 0 to 0.7, the mean absolute difference (MAD) of our proposed system decreases. Therefore, we use $\lambda_1 = 0.7$ and $\lambda_2 = 0.3$ as the combining coefficient. It is worth noting that when $\lambda_1 = 0$ and $\lambda_2 = 1$, our proposed system uses AoA information only, and when $\lambda_1 = 1$ and $\lambda_2 = 0$, our proposed system uses CIR information only for positioning.

The CIR and AoA metric has different positioning capabilities. Fig. 7 shows the MAD of different regions when only CIR and AoA were used. As shown in this figure, our CIR and AoA metric has different localization performance when the user is at different locations, e.g, the localization performance of row one column two is quite different from that of row seven column nine. This is due to the fact that we collect fingerprints on the grids of equal distance and these reference points may have different multipath propagation.

Authorized licensed use limited to: University of Electronic Science and Tech of China. Downloaded on July 18,2022 at 08:12:10 UTC from IEEE Xplore. Restrictions apply.

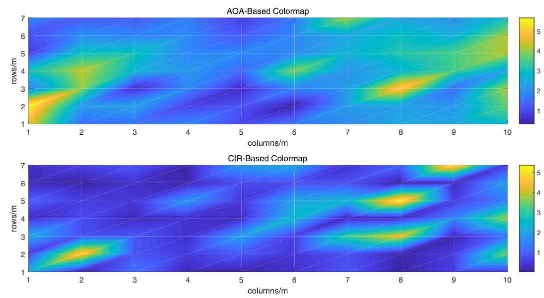

Fig. 7: Location error with CIR and AoA

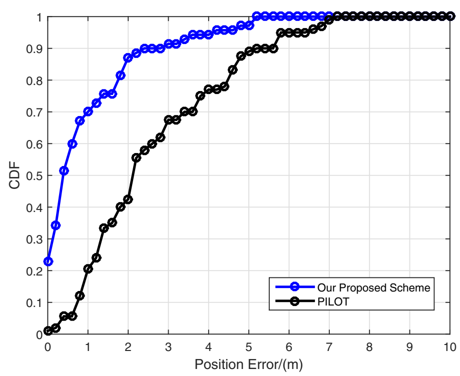

Fig. 8: Error Performance Comparison of our proposed method and PILOT

Fig. 8 compares the localization performance of our proposed system with the PILOT, a CSI based DFPL [17] which has been implemented by us. As shown in Fig. 8 our scheme performs better than PILOT in both X and Y directions. The median of the MAD of our proposed scheme is approximately $0.5m$, while that for PILOT is approximately $2m$, 75% worse than our proposed scheme.

V. Conclusion

The use of CIR and AoA as the signature of localization system is able to improve the accuracy of indoor positioning system. We proposed a DFPL system that uses the fingerprint that incorporates the CIR and AoA information. The system, which uses the JSD between two distributions and AoA cluster centers as the distance metric, demonstrates better position accuracy than conventional DPFL which only uses CIR information.

References

[1] K. Wu, J. Xiao, Y. Yi, M. Gao, and L. M. Ni, "FILA: Fine-grained indoor localization," *Proceedings - IEEE INFOCOM*, pp. 2210–2218, 2012.

[2] A. Rai, K. K. Chintalapudi, V. N. Padmanabhan, and R. Sen, "Zee: Zero-Effort Crowdsourcing for Indoor Localization," *Proceedings of the 18th annual international conference on Mobile computing and networking - Mobicom '12*, p. 293, 2012.

[3] Z. Yang, C. Wu, and Y. Liu, "Locating in fingerprint space: Wireless indoor localization with little human intervention," *Proceedings of the Annual International Conference on Mobile Computing and Networking*, pp. 269–280, 2012. [Online]. Available: http://dx.doi.org/10.1145/2348543.2348578

[4] C. Wu, Z. Yang, Y. Liu, and W. Xi, "WILL: Wireless indoor localization without site survey," *IEEE Transactions on Parallel and Distributed Systems*, vol. 24, no. 4, pp. 839–848, 2013.

[5] G. Shen, Z. Chen, P. Zhang, T. Moscibroda, and Y. Zhang, "Walkie-markie: Indoor pathway mapping made easy," *Proceedings of the 10th USENIX conference on Networked Systems Design and Implementation*, pp. 85–98, 2013.

[6] Y. Chapre, A. Ignjatovic, A. Seneviratne, and S. Jha, "CSI-MIMO: An efficient Wi-Fi fingerprinting using Channel State Information with MIMO," *Pervasive and Mobile Computing*, pp. 1–15, 2015. [Online]. Available: http://linkinghub.elsevier.com/retrieve/pii/S1574119215001406

[7] Z. P. Jiang, W. Xi, X. Li, S. Tang, J. Z. Zhao, J. S. Han, K. Zhao, Z. Wang, and B. Xiao, "Communicating is crowdsourcing: Wi-Fi indoor localization with CSI-based speed estimation," *Journal of Computer Science and Technology*, vol. 29, no. 4, pp. 589–604, 2014.

[8] J. Wilson and N. Patwari, "Radio Tomographic Imaging with Wireless Networks," *IEEE Transactions on Mobile Computing*, vol. 9, no. 5, pp. 621–632, may 2010. [Online]. Available: http://ieeexplore.ieee.org/lpdocs/epic03/wrapper.htm?arnumber=5374407

[9] K. El-Kafrawy, M. Youssef, A. El-Keyi, and A. Naguib, "Propagation modeling for accurate indoor WLAN RSS-based localization," *IEEE Vehicular Technology Conference*, no. April 2016, 2010.

[10] H. Shin, Y. Chon, Y. Kim, and H. Cha, "MRI : Model-Based Radio Interpolation for Indoor War-Walking," *IEEE Transactions on Mobile Computing*, vol. 14, no. 6, pp. 1231–1244, 2015.

[11] Y. Chapre, A. Ignjatovic, A. Seneviratne, and S. Jha, "Csi-mimo: Indoor wi-fi fingerprinting system," in *Local Computer Networks*, 2014, pp. 202–209.

[12] K. Qian, C. Wu, Z. Yang, Y. Liu, and Z. Zhou, "PADS : Passive Detection of Moving Targets with Dynamic Speed using PHY Layer Information," in *2014 20th IEEE International Conference on Parallel and Distributed Systems (ICPADS)*, 2014, pp. 1–8.

[13] W. Liu, X. Gao, L. Wang, and D. Wang, "Bfp: Behavior-Free Passive Motion Detection Using PHY Information," *Wireless Personal Communications*, 2015. [Online]. Available: http://link.springer.com/10.1007/s11277-015-2438-7

[14] a.a.M. Saleh and R. Valenzuela, "A Statistical Model for Indoor Multipath Propagation," *IEEE Journal on Selected Areas in Communications*, vol. 5, no. 2, 1987.

[15] M. Kotaru, K. Joshi, D. Bharadia, and S. Katti, "Spotfi:decimeter level localization using wifi," *Acm Sigcomm Computer Communication Review*, vol. 45, no. 5, pp. 269–282, 2015.

[16] D. Halperin, W. Hu, A. Sheth, and D. Wetherall, "Tool release:gathering 802.11n traces with channel state information," *Acm Sigcomm Computer Communication Review*, vol. 41, no. 1, pp. 53–53, 2011.

[17] J. Xiao, K. Wu, Y. Yi, L. Wang, and L. M. Ni, "Pilot: Passive Device-Free Indoor Localization Using Channel State Information," *2013 IEEE 33rd International Conference on Distributed Computing Systems*, pp. 236–245, 2013. [Online]. Available: http://ieeexplore.ieee.org/lpdocs/epic03/wrapper.htm?arnumber=6681593

Authorized licensed use limited to: University of Electronic Science and Tech of China. Downloaded on July 18,2022 at 08:12:10 UTC from IEEE Xplore. Restrictions apply.